# Experiences with Raytheon Si:As IBC detector arrays for mid-IR interferometric observations

S. Ligori, U. Graser, B. Grimm, R. Klein
Max-Planck-Institut für Astronomie, Heidelberg

**ABSTRACT**

Interferometric observations at 10 micron combine the difficulties of the relatively new interferometric techniques with the problems of overcoming the strong and highly variable thermal background which are typical of thermal infrared observations. In particular, the detector subsystem must comply to strict requirements in terms of stability, of read noise, and of read out speed. Here we present the results obtained during laboratory test of MIDI, the Mid-IR interferometric instrument for VLTI. We selected as detector for the MIDI instrument a Raytheon 320x240 IBC array. We will discuss some of the aspects of the foreseen operation of MIDI, and the methods adopted to implement those on our detector system. We will show our results on detector stability, on its performances (in particular Quantum efficiency and read-out noise), and on the reaction to high fluxes. By using the possibility of hardware windowing, frame times of the order of 2 ms can be reached. Finally, we will show the characteristics of the detector when used in interferometric mode during tests of the whole MIDI instrument with both monochromatic and broad band calibration sources.

**Keywords:** Interferometry, Mid-IR, Electronics, Infrared Detectors

## 1. INTRODUCTION

Thermal infrared astronomical observations from ground-based telescopes are normally complicated by the presence of a strong background flux, coming from both the atmosphere and from the telescope itself. The backgound flux is also strongly variable and therefore it is needed to monitor its evolution at relatively high frequency. One of the main requirements of a detector system for Mid-IR astronomical observations is a high read-out speed, in order to avoid saturation of the detector caused by the high background and to enable the observer to use appropriate techniques for monitoring and removing any fluctuations due to variation in the background or to drifts in the detector and the read-out electronics.

Interferometric observations also require high read-out speeds, in order to overcome the effects of the atmosphere on the fringe position.
The detector subsystem of MIDI, the Mid-IR instrument of the Very Large Telescope Interferometer (VLTI)[1,2] has been designed to reach high frame rates while keeping, at the same time, a low read noise.
In addition, due to the nature of the measurements themselves, the detector subsystem must provide means for synchronization with the other components of the instrument. In particular, the movement of the MIDI internal delay lines must be synchronized with the acquisition of frames on the detector, in order to relate precisely the data obtained with the value of the Optical Path Delay (OPD) at that moment.

The requirements for the MIDI Read-Out Electronics (ROE) are the following:

- read the detector at high speed and with low noise;
- provide a reliable data transfer to the Detector Workstation (DWS), which is designed to perform some real-time preprocessing of the data and give a feedback to the other MIDI subsystems[4];
- synchronize efficiently and reliably with the other components of the instrument, via communication with the DWS and the Delay Line Local Control Unit (DL-LCU).

The MIDI ROE has been developed at MPIA; most of its components are, or will be, used by other IR instruments developed in Heidelberg. The design and early tests of the MIDI detector subsystem have been described previously[3]. In the following we will briefly review the current system architecture, and the results of the laboratory tests which will lead to the tests for the Preliminary Acceptance in Europe (PAE).

Send correspondence to: Sebastiano Ligori, Max-Planck-Institut für Astronomie, Königstuhl 17, 69117 Heidelberg, Germany; e-mail: ligori@mpia.de

We will concentrate in particular on the most critical aspects related to interferometric observations, such as detector stability, available observing modes, read-out noise and speed, as well as sensitivity. We will describe the handshake mechanism used to synchronize the detector read-out with the motion of the MIDI fast delay lines, and its performances in terms of temporal stability and accuracy.

## 2. THE DETECTOR

The MIDI detector is a Raytheon 320x240 pixel[2] Si:As Impurity Band Conduction (IBC) hybrid[5]. It has a pixel size of 50 µm with an active area of 98 %. The gain can be switched between a low and a high value, with a ratio of about 3. The read-out multiplexer implements an on-chip Correlated Double Sampling (CDS) feature.
There are two different operational modes: "integrate while read" (IWR) and "integrate then read" (ITR). In both modes, the detector is read-out row by row; in IWR the rows which are not selected for read-out are constantly integrating; the integration time is given therefore by the interval between two reads of the same row. In ITR mode, the integration of the photocurrent into the integration capacitance is controlled by switching the detector bias; the integration time is therefore defined by the time in which the photocurrent is actually collected in the integration capacitance. After integration, the detector is read-out. As it is clear from the above description, the main differences between the two modes are the following:

- IWR allows for the higher frame rates, while ITR can provide the shorter integration times. On the other hand, at short integration times using ITR the efficiency tends to be very small;
- in ITR mode all the pixels integrate during the same time interval, while in IWR, although the integration time is the same, the pixels are not integrating simultaneously. This can be an undesirable feature for interferometric observations, in which the OPD is modulated during the read-out, but the effect can be easiliy calibrated off-line.

Since MIDI operations are characterized by a wide spectrum of background fluxes, ITR mode will be mostly used in high-background applications, while the more time-efficient IWR mode will be used in setups characterized by a lower background flux.

Hardware windowing is implemented for both observing modes. In the Raytheon detector windowing can be performed only row by row; selection of columns can only be obtained by software. In the case of MIDI, in most of the observing modes only a fraction of the detector is actually illuminated, so that hardware windowing can be effectively used to reduce the amount of data transferred to the Detector Workstation (DWS) and the frame time.

## 3. THE READ-OUT ELECTRONICS

A scheme of the ROE architecture is shown in Fig. 1. Since the MIDI read-out electronics architecture has been already described in a previous paper[3], we will discuss here only the main modifications to the hardware.
The ROE is composed of a Front End part (providing biases and clocks to the detector, and receiving the output signals), attached directly to the dewar, close to the detector, and an Electronics Box containing the Data Acquisition and Control modules. The ROE is then connected to the DWS (a SUN Enterprise 450) which takes over and performs some limited near-real-time preprocessing of the raw data, and transfer the data to the Near Real Time Server (NRTS) on the Preprocessing Workstation. The DWS receives from the Observation Software (OS) the parameters needed for the observation, and forwards the settings to the ROE via a serial line.

After readout, the frames are sent from the Electronics Box to the DWS via a double fiber optics link to two PCD 60 parallel I/O boards on the DWS. The double data path was introduced to reduce the noise at high data transfer rate.

The boards shown in Fig. 1 are shortly described in the following.

### 3.1 Boards at the dewar

#### 3.1.1 Clock Driver Board

The clocks and biases signals from the clock-control board are separated and converted to their specific voltage levels in this board. The upgrade of the clock driver board allowed us to manage a larger number of clocks, which turned out to be very useful when operating such a complex detector.
The clock-driver board receives the clock patterns from the Clock Control Board contained in the Read Out Electronics box and switches the appropriate voltage levels which are then sent to the detector. To avoid possible ground loops the incoming clocks are then decoupled by means of optocouplers.

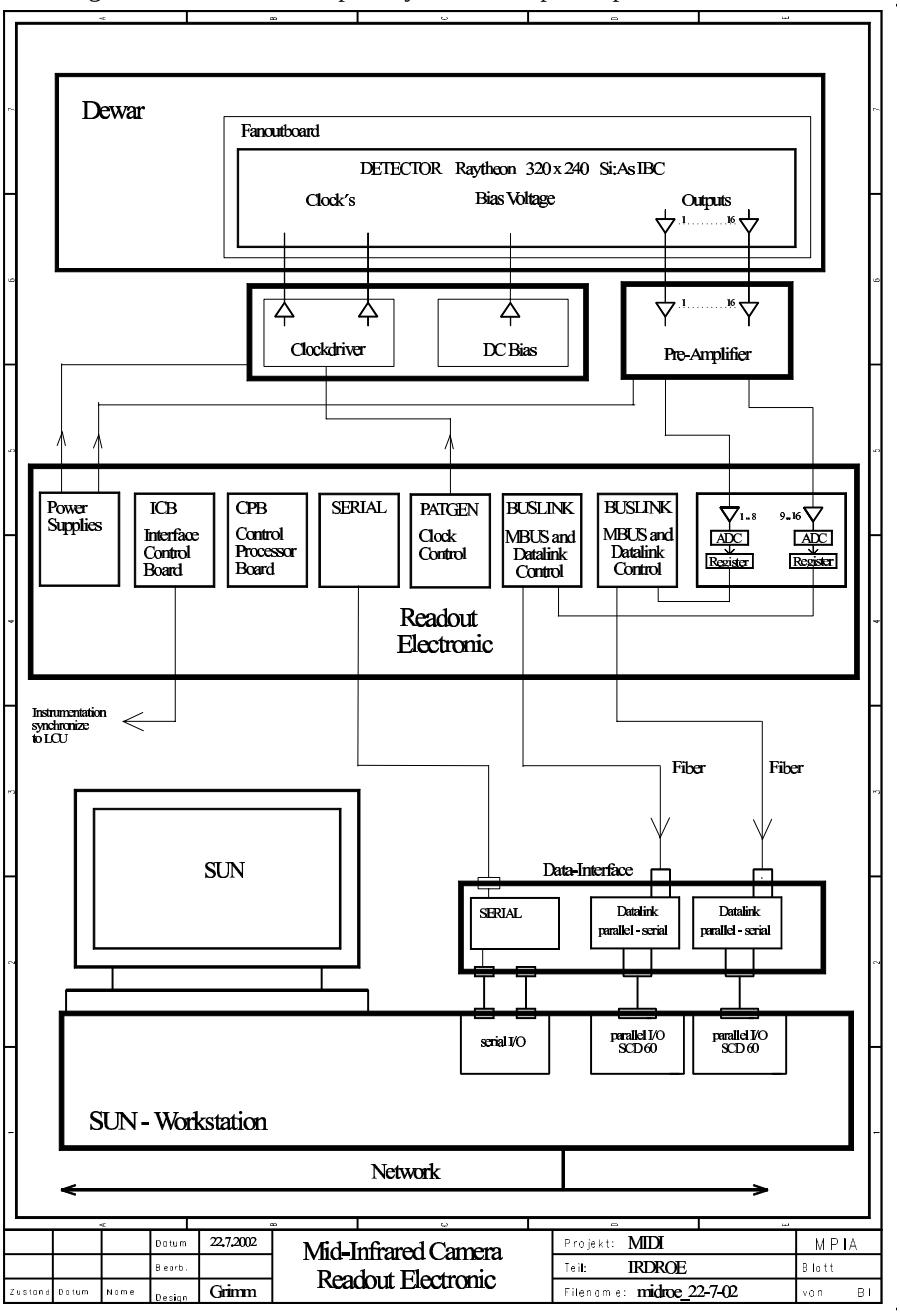


**Figure 1: Schematics of MIDI Read-Out Electronics**

The voltages are provided by the bias board and switched to the detector through analog switches; the switch command itself is coming from the optocouplers.

### 3.1.2 Preamplifiers

The preamplifiers perform the first amplification of the detector signal, in order to fit the dynamic range of the analog-to-digital converters (ADC). The preamplifier board is attached directly to the dewar in order to minimize the length of the wires from the detector outputs to the preamplifiers.
The detector can operate both in 16- and 32-outputs mode: in 32 outputs mode, to a given pixel time corresponds a data rate per ADC which is half of that in 16 outputs mode. However, in the present implementation of MIDI electronics we decided to work in 16 outputs mode.
Since the detector signal is superimposed on a common mode voltage, an offset voltage must be provided to compensate it before to go to the ADCs. One offset voltage source can provide variable voltage to 8 amplifier stages; the voltage is in fact distributed to 8 adjustable voltage dividers, so that each output can be compensated individually. In order to distribute the load evenly between both sides of the ±5 V Power Supply (PS), the offset is trimmed in such a way that for the whole input range the output swing goes from -2.5 V to +2.5 V. This board is also an upgraded version of the one used in the first tests; in particular, it provides both a global offset adjustment and separated adjustment for each channel. It provides also the possibility to switch between two different gain values, in order to map the whole output swing of the detector or only a smaller portion. In high gain mode, there is in addition the possibility to select two values for the offset.

### 3.1.3 Bias Board

The bias board provides various (negative) voltage levels:

- voltage for the digital clocks;
- power supply for the digital circuitry on chip;
- power supply for the source followers on chip;
- voltages for the remaining biases.

The voltages are generated from a +2.5V reference source. This voltage is fed to two opamps which feed with 23 adjustable potentiometer. The output voltages are filtered by a special RC-combination which has a low impedance over a wide frequency range.
For additional low frequency filtering a 100 µF Tantalium capacitor is added. To further secure the outputs against static discharges, fast reacting voltage suppressor diodes are provided.
The bias board provides also 4 switched voltages. In these cases an analog switch has been used, with the switch command provided by the clockboard.

## 3.2 Boards at the Electronics crate

### 3.2.1 Interface Control Board

The Interface Control Board (ICB) contains analog, digital, and RS232 connectors for monitoring, recording and control of system parameters. The external trigger signal from the DL-LCU needed for the synchronization mechanism (see Sec. 4) is received by one of the digital I/O lines of the ICB.

### 3.2.2 Control Processor Board

The Control Processor Board (CPB) controls the activities of the whole ROE.
This is done by means of a Texas Instruments Digital Signal Processor (DSP) TMS 320C30.
The board includes 256Kx32 bits of programmable memory (EPROM) and 256Kx32 bits of static RAM.

### 3.2.3 Clock-control board (PATGEN)

The selected read-out pattern is loaded by the DSP into the RAM of the Clock Control Board (PATGEN). A number of different patterns can be loaded on the DSP and can be used to implement the different read-out modes; the clock patterns are loaded via the serial port of the CPB from the detector workstation, giving to the system a high flexibility.
In addition to provide the clocks for the operation of the detector, the PATGEN board uses two of its clocks to generate a synchronization signal to be sent to the DL-LCU and to produce the End-of-file marker which is used to check the data integrity (see Sec. 4).

### 3.2.4 ADC boards

The detector signals coming from the pre-amplifiers are amplified and digitized by 2MHz 16 bit ADCs (Analogic ADC 4322A). Each board has 8 ADCs, and up to 4 boards can be used. The signal coming from the preamplifier is routed through a coaxial cable with a characteristic impedance of 50 Ω, so the input of the ADC-Board terminates the cable with a 50 Ω resistor. Following this the signal is fed into a LRC low-pass filter, a 2nd Bessel filter with a corner frequency of 2.4 MHz.

After the low-pass filter, the signal is amplified by a factor 2 to compensate for the loss due to the voltage divider formed by the two terminating resistors. The output of each amplifier goes to jumpers by means of which the input range of the ADC can be set. Since the signal from the preamplifiers comes with a range of ±2.5 V, the ADC range is fixed to this value.

The outputs of the ADCs are latched with End of Conversion Pulses into 2x8 D-Type Flip-Flops with 3-State outputs. The Start Convert Signal is generated on the Clock Control Board together with the other clock pulses.

This signal is sent to the BUSLINK board, which creates a Master Start Convert Pulse. The Start Convert Signal can be used to control the Analog to Digital conversion and therefore the data output; disabling the corresponding clock, one can run the detector continuously without producing data, implementing in this way the idle cycles which are necessary between the observations to keep the detector thermally stable.

All ADCs in each board start the conversion simultaneously; the End of Conversion (EOC) signals, which can come at slightly different times respect to each other, are combined in a single EOC which is sent to the BUSLINK board through the Backplane Connecting Board. The BUSLINK board then will start to read the data and to sent them to the DWS.

### 3.2.5 BUSLINK board and Backplane Connecting Board

The BUSLINK boards control the read-out of the ADC boards and the data transfer via fiber optics (DATALINK) to the data-interface on the DWS. As mentioned earlier, we use two BUSLINK boards in parallel for the two halves of the array, which uses two distinct Backplane boards.

Each of the BUSLINK boards receives the Start Conversion Pulse and generates a Master Start Convert Pulse which is sent to the Backplane Connecting Board.

The Backplane Connecting Board links the clocks with the ADC Boards; it receives the Master Start Convert pulse and transfers it to the ADCs.

### 3.2.6 Serial communication board

The communication with the DWS is performed with this serial card which provides a fiber connection to the data interface on the DWS at a maximum speed of 115200 bps.

### 3.3 Boards at workstation

### 3.3.1 Data Interface

The Data interface box contains a transceiver to convert the fiber input from the Serial communication board into electrical signals which are fed into a serial port on the DWS. In addition to that it contains two DATALINK boards which receive the detector data and send them via two PCD 60 boards to the DWS. As already mentioned, with respect to the original design the main change is the doubling of the data path.

## 4. SYNCHRONIZATION

A critical issue in operating MIDI is to synchronize the detector read-out (start and end of each elementary integration, start and end of the read-out phase) with the rest of the MIDI instrument, in particular with the Delay lines which are used to scan the fringe pattern, and which are controlled by the Delay Line Local Control Unit (DL-LCU). Since the entire observation needs to be scheduled in advance to manage the different operations on the MIDI instrument as well as on the VLTI system, it is also necessary to be able to stop the idle cycles of the ROE and start a data-taking sequence in a fixed (and as small as possible) amount of time. The ROE must therefore be able to react to an external trigger signal provided by the Intrument Workstation (IWS).

Moreover, a synchronization mechanism is necessary in the data path between the ROE and the DWS, to allow correction for incomplete trasmission of data.
Two mechanisms are implemented to meet these goals. In normal operation, after setting up the required read-out mode and integration time, the detector will be read-out without actually sending data (idle cycles). This is necessary in any case, to ensure thermal stability of the detector before taking data. The idle cycles can be interrupted at any moment by a trigger signal sent by the DL-LCU; the time required to stop the idle cycles, enable the data conversion on the ADCs and start a data-taking sequence is about 1ms. Prior knowledge of the exact frame time is necessary to schedule the observation, while the movement of the piezo is synchronized by means of a status line going from the ROE to the DL-LCU, providing information on the phase of the read-out. This status line is driven by one of the clocks produced by the PATGEN board, and therefore can be managed by modifying the clocking pattern. In Integrate-then-read (ITR) mode, the piezo will be moved during the read-out time, and the status line provide information on the end of the integration and therefore the start of the read-out. Since the read-out time depends on the hardware windowing setup chosen, a dynamic computation of the timing used is implemented. If necessary, the frame time will be adjusted to better fit the other parameters of the observations (e.g. chopping frequency). In ITR mode this can be done by increasing the global reset phase which occurs before the integration; in this way the selected integration time can be kept. In IWR mode, since there is no global reset, a rounding up of the integration time will be necessary.

## 5. DETECTOR PROPERTIES

Since the begin of 2001, a Science Grade detector has been tested at MPIA in order to optimize both the operation of the ROE and the performances of the detector itself. Here we remind the main figures of merit for this kind of detectors as reported by the manufacturer:

- Full well capacity: $1.0\ 10^7$ / $3.0\ 10^7$ $e^-$ (respectively in high gain and low gain mode)
- Read out noise < 1000 $e^-$ (in high gain mode)
- Quantum efficiency > 40%

The performance goals of MIDI were set according to these values. In the following we discuss the results of our tests on these main characteristics.

### 5.1 Full well capacity

The full voltage swing measured between starvation and saturation is 1.8 V; this corresponds to $9.46\ 10^6$ $e^-$. The output is linear within about 3% up to $5.8\ 10^6$ $e^-$.

### 5.2 Read-out noise

The read-out noise in our case appears to be mainly originated in the Read-Out Electronics. In addition to this contribution we found a component apparently due to an intrinsic characteristic of the detector, and related to the clocking which is used to read-out the device. In the normal read-out sequence, in fact, the output stage level shifter, which is controlled by two switched biases (VOFFSET and VCLOUT) is reset at the beginning of every frame by applying the above mentioned biases to the two sides of a capacitor. We found that, following this mode, there is a frame to frame variation in the offset, which is also different for the different output channels. This causes relatively large variations; this effect is larger in the central channels, as can be seen in Fig. 2 which is a map of RON on a sequence of 500 frames at 0 integration time.

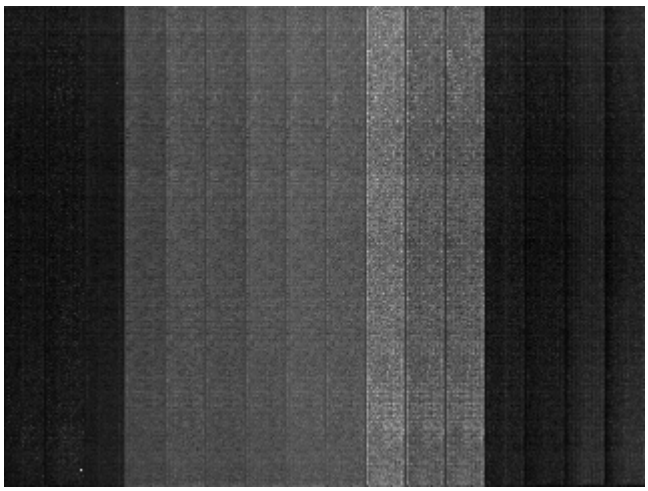

**Figure 2: Map of read-out noise over a 500 frames sequence**

The histogram of the RON distribution corresponding to the map in Fig. 2 is shown in the left plot of Fig. 3, where one can notice that:

1. there are two main population: this is caused by the offset change caused by clocking PCLOUT;
2. most of the pixels are anyway below 1000 e- RON, so within our design goal.

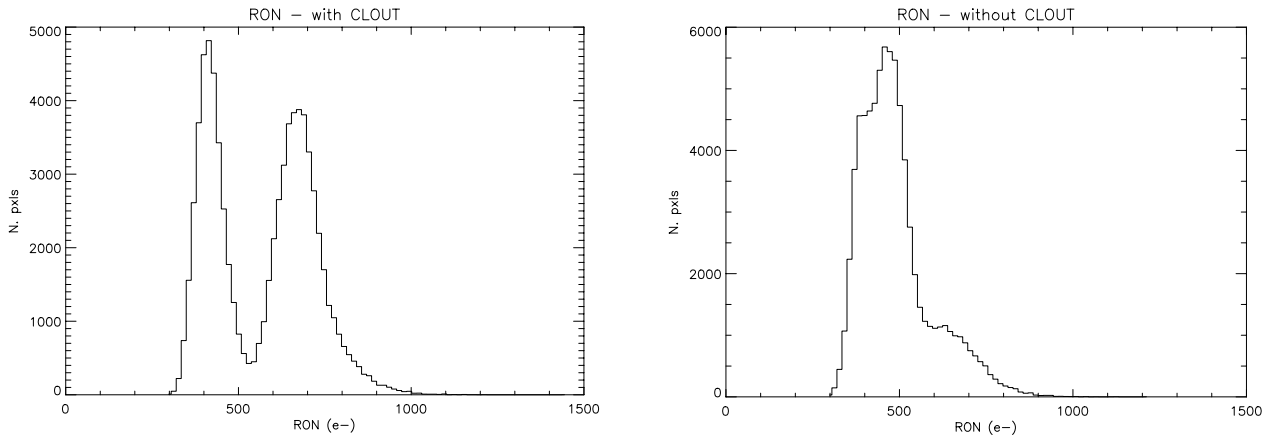


**Figure 3: Histograms of read-out noise. Left is for a clocking with CLOUT switched on every frame, right is without CLOUT pulse**

An improvement in RON can be obtained by avoiding to clock PCLOUT every frame. In this case the output level can drift with time, even if we observed that there are no noticeable drifts on timescales of several tens of minutes, but there are no frame to frame variations in offset. This translates in better noise performances, as can be seen in the right hand plot of Fig. 3. If PCLOUT is not clocked every frame, it must be anyway reset from time to time. We provide the possibility of running a few frames in a mode in which PCLOUT is enabled, and these additional frames can be included in the observing sequence. It is any case possible to efficiently remove this effect offline, provided that we store every individual frame and that there are areas on the detector which are not illuminated, which is mostly the case in MIDI operation.

### 5.3 Quantum efficiency

As recalled previously, the design value for the QE provided by Raytheon is >40% at peak. We measured, in the N band, a value of about 37%. This is roughly within specifications, although lower than the value measured with the same chip by the manufacturer.

### 5.4 Dark current

We could not make accurate measurements for the dark current because of the instrumental background in the MIDI dewar. We would not be able in any case to measure the value of 100 e-/s provided by the manufacturer. We can set an upper limit for the dark current at 10K (the normal operating temperature in MIDI) of 1.0 $10^5$ $e^-$/s. This value, even if much larger than the specification, should not be a major concern in MIDI, because of the very short integration times (maximum 25 ms) imposed by the need to overcome the fringe motion caused by atmospheric turbulence and, in many observing modes, to avoid saturation due to the background flux.

### 5.5 Frame rates

The minimum read time for a full frame is 6.2 ms. This time is in part due to the clocking of the pixels of each row (20 pixels per output at 750 ns per pixel, giving a total of 15 µs per row, and 3.6 ms per 240 rows), and in part to the time needed to perform the on-chip CDS and to load the signal in the Sample and hold circuitry. This frame time would be too long for some of the foreseen observing modes, but we can exploit the fact that, in the case of MIDI, a large part of the detector area is in fact not illuminated. Using the possibility of row selection given by the architecture of the MUX, we can skip the undesired rows and reduce significantly the frame time. In addition, hardware and software windowing allow us to reduce the amount of data flowing through our pipeline, thus reducing the load on the system.

Hardware windowing has been tested in both snapshot and "Integrate-while-read" mode. In particular, in the latter mode, one can reach the highest frame rates, since the integration is performed during the read-out and there is no additional overhead due to the global reset and integration phase which is present in snapshot operation. In dispersed mode, a frame time of about 2ms can be reached using appropriate hardware windowing.

### 5.6 Excess noise at high counts

In a shot noise-dominated regime, the noise should be proportional to the square roots of the average number of counts. In the case of the MIDI detector, this seems not to be the case. Starting at relatively low counts (20000 ADUs) we observe in fact a deviation from the poissonian relationship. At 30000 ADUs, the noise is 30% higher than the foreseen shot noise. This of course limits our SNR by a significant amount. The origin of this effect is not known at present, but it appears to be less important when relatively long integration times can be used.

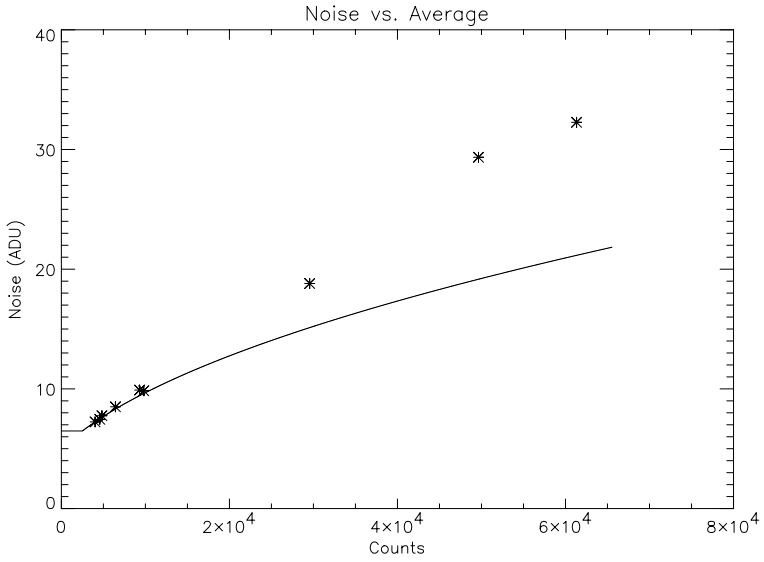


**Figure 4: Noise vs. average at different flux levels. Each point represents the mean value computed on the pixels in a 10x10 area**

### 5.7 Offset variations in presence of bright sources

Another undesired effect is detected when observing bright objects, i.e. objects significantly brighter than the background. In Fig. 5 we show the raw images from the detector with (Fig. 5 a) and without (Fig. 5 b) the calibration blackbody. In Fig. 5 c) it is shown, with high contrast, the difference of the previous images.
As it is illustrated in Fig. 5, we see three kind of artifacts:

1. offset variations which interest a whole channel
2. offset variations which interest only the columns where the peak is located
3. offset variations in all the other outputs, in locations corresponding to the bright source.

The amount of offset change is of the order of a few percent. While this is significant for very bright source, the disturbance due to these effects becomes smaller than the shot noise in many real cases, in which the source is very faint when compared to the background.

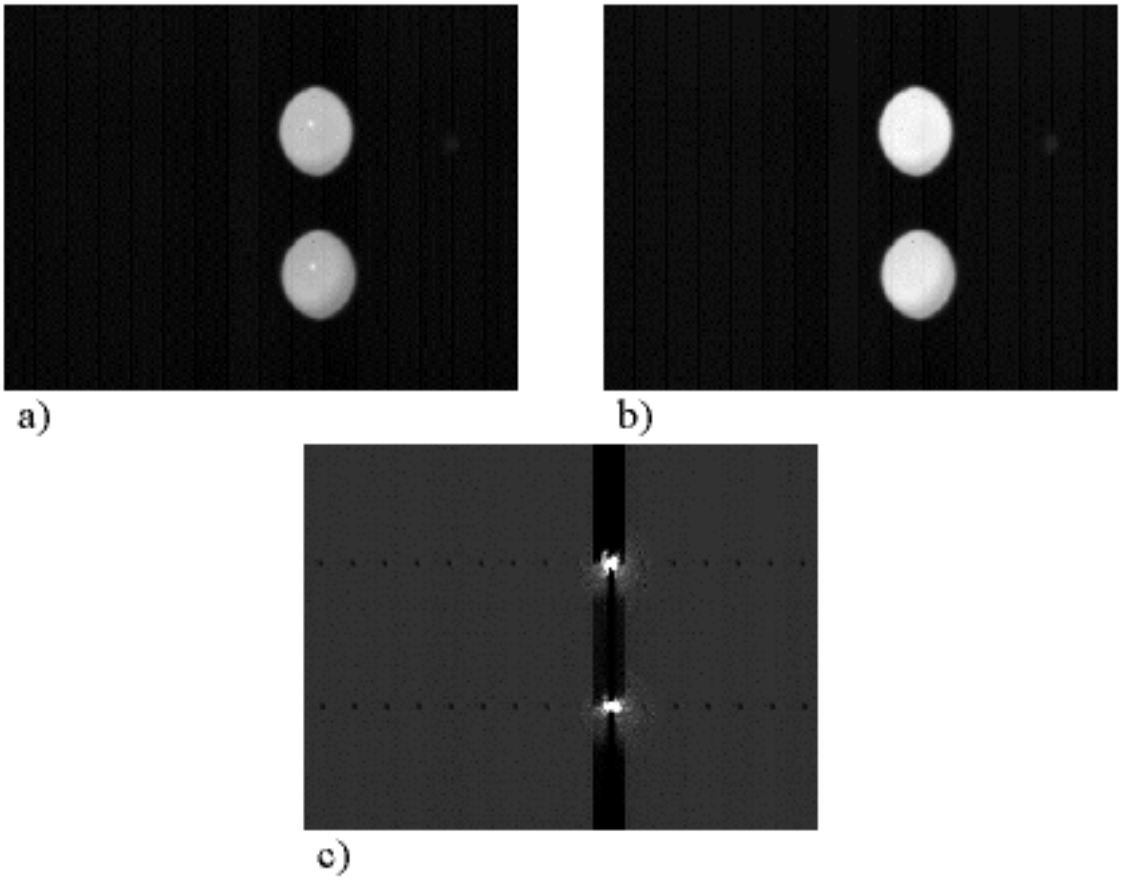


**Figure 5: Offset variations in presence of bright sources**

This effect is already known from experiences of other groups using Raytheon arrays, but no solution has been found. A possible solution is to sample the value of CLOUT and CLCOL in addition to the output level, but this approach would imply in our case a very long read-out time, which cannot be accepted.
Offline data reduction can be used to partially correct these effects, at least for 1. and 2. Removal of effect 3. is difficult, and it is impossible in the case of dispersed images.
The effect 2. (on the same column of the peak) is normally at a level of about 3% of the peak itself, while the offset change on the channel is about 10 times smaller. The effect 3. (crosstalk on all the channels) is also of the order of 0.3% of the peak counts, and affects, as it can be seen on Fig. 5, only a few pixels, corresponding to the main peak.

With the possible exception of extremely bright objects, correcting offline for offset and sky variations will be sufficient to reach the required accuracy in visibility.

**5.8 Persistency effects and thermal stability**

As already mentioned, before taking data with a given setup it is necessary to run some idle cycles with the same parameters (instrument setup, read mode, and integration time) in order to reach a good thermal stability on the detector. Experience shows that 100 frames are the minimum number necessary to reach this goal . This corresponds, in most of our observing modes, to a few seconds, so it is normally not a problem to have this time during preparation for an observation. However, this requirement puts restrictions on more complicated data-taking sequences (in which, for instance, the integration time must be modified very often) because the overhead then can become quite large. Persistency effects are seen when observing very bright sources, with the detector saturated or close to saturation. In this case, after removal of the source, a time of the order of a couple of minutes can be necessary to recover the previous background image. These effects must be taken into account, but they will likely affect observations only in a few cases of extremely bright objects.

## 6. INTERFEROMETRIC TESTS

In the previous sections, we described the characteristics of the MIDI detector as a standalone device. We discussed the performances of the detector and we showed that, with the exception of an excessive noise at high counts, they are within the specifications. From the end of 2001 to the present day, this detector has been used extensively to test the operation of the MIDI instrument as a whole. Here we present some of the results, showing how the characteristics of the detector impact the global perfomance of the MIDI instrument.

**6.2 First interferometric fringes**

On October 31st, 2001, we obtained the first fringes with MIDI. A sequence of images from that day is shown in Fig. 6.

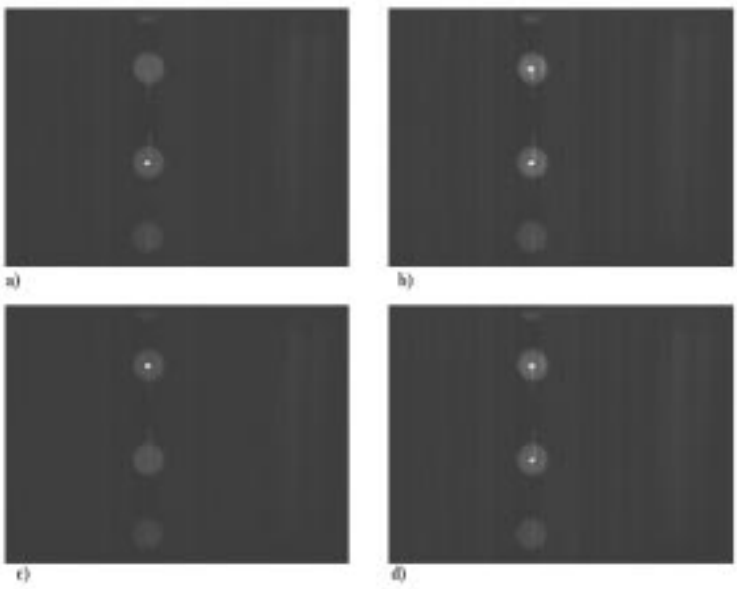

**Figure 6: First fringes with MIDI**

In this picture one can see the light from our laser source, which is split before the entrance into the dewar in two beams, interfering constructively in one beam while interfering destructively in the other beam. The different pictures are taken by moving the piezo by roughly one quarter of a wavelenght per step (about 2.6 µm, since the wavelength of the laser is 10.6 µm). These are all raw frames, and no offset change effect is visible. Analyzing these and similar data, one can calculate an instrumental visibility of 80%. The lowest aperture is one of the photometric channels, the other

one being barely visible at the upper edge of the frame. This effect, due to a misaglinment in the cold optics, has been later corrected.

**6.3 White light fringes**

Here we show an example of white light fringes obtained with an additional dispersing unit (a grism with resolution R=230).

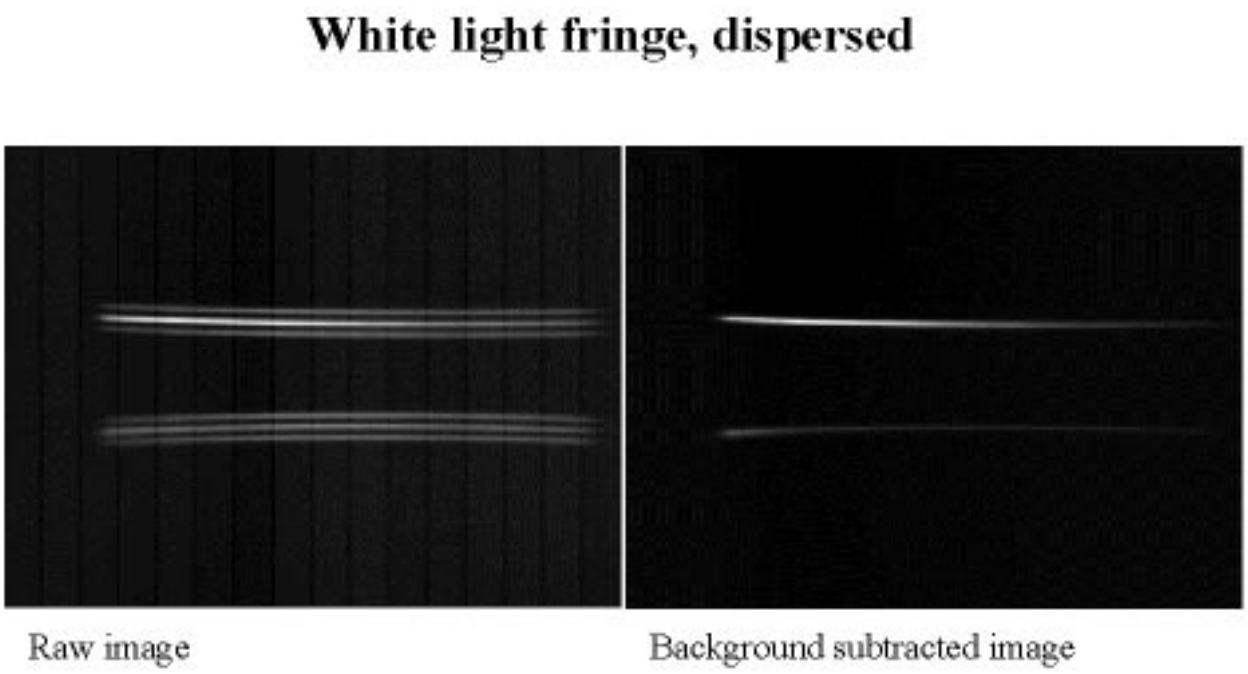


**Figure 7: white light fringe**

In this figure we show the raw image on the left and the same image after subtraction of a reference background image. This image represents one of a sequence, during which the MIDI delay line translation stage was scanning a range of Optical path differences. As can be seen clearly, in Fig. 7 the signal is at its maximum in one of the interferometric channels (the upper one) and is at the minimum in the other one. This is what is expected at zero OPD. In the raw image, in addition to the two central pinholes with the light from the calibration blackbody, one can see two additional pinholes which can be used to monitor the background variations. In fact, these pinholes disappear almost completely when removing the reference image.

The image shown here was obtained in full frame mode. As it can be seen, only a small portion of the detector is illuminated; by selecting only the illuminated rows on the detector, a frame time of 1.4 ms has been reached with this configuration.

In Fig. 8 is shown a plot of a fringe scan in one of the spectral channels of Fig. 7. Due to the narrow bandwidth, fringes are visible over many wavelengths before the zero OPD position. The offset change effect cannot be shown in this image because of its small contribution with respect to the large signal swing. Not taking into account this effect, however, one can produce an error of about 4% in the estimated visibility.

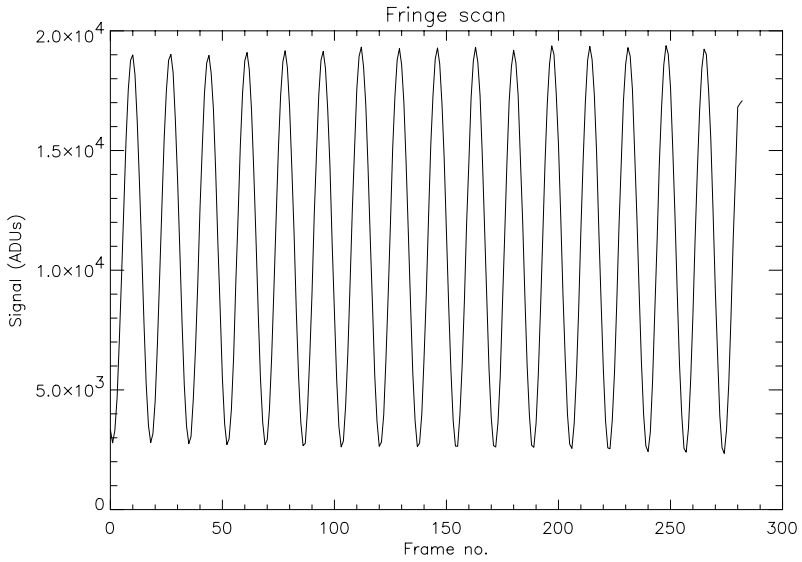


**Figure 8: Fringe scan in one spectral channel**

## 7. CONCLUSIONS

Interferometry at 10 µm is a very difficult challenge, with many aspects still unknown. For instance, the amount, the behaviour and the impact of instrumental background from the VLTI will be known only with the first commissioning tests on Paranal. The detectors for this wavelength range are also quite difficult to operate, especially considering the stringent requirements imposed by such a complex instrument as MIDI. We have shown here that most of the main characteristics of the MIDI detector subsystem are matching specifications, although two major problems still remain, namely the excess noise at high counts and the undesired effects on the offset in the presence of a bright source. This latter problem, though, is not likely to play a major role in normal conditions, since the expected background level will almost always dominate the observed source. A big effort is now placed in understanding and possibly reducing the excess noise.

## ACKNOWLEDGEMENTS

The authors wish to thank the staff of the MPIA's electronics workshop for their contribution to the realization of the MIDI ROE.

## REFERENCES

1. Ch. Leinert et al., *10 µm interferometry on the VLTI with the MIDI instrument: a preview,* Proc. SPIE, 4006, p. 43, 2000
2. Ch. Leinert et al., *The 10 µm instrument MIDI - getting ready for observations on the VLTI,* these proceedings
3. S. Ligori, U. Graser, B. Grimm, and R. Klein, *Design and tests of the MIDI read-out electronics,* Proc. SPIE, 4006, p. 136, 2000
4. S. Hippler, W. Jaffe, R. Mathar, C. Storz, K. Wagner, W. D. Cotton, G. Perrin, and M. Feldt, *MIDI: controlling a two 8-m telescope Michelson interferometer for the thermal infrared,* Proc. SPIE, 4006, p. 92, 2000
5. A. D. Estrada and others, *Si:As IBC IR focal plane arrays for ground-based and space-based astronomy,* Proc. SPIE, 3354, p. 99, 1998